

# Geometric Approach to Power Analysis in Non-Sinusoidal and Unbalanced Multiphase AC Circuits in the Frequency Domain

Francisco G. Montoya, Jorge Ventura, Francisco M. Arrabal-Campos and Alfredo Alcayde

**Abstract**—This research paper presents a new approach to power definitions in multiphase AC circuits in the frequency domain from a purely geometric approach. The theoretical foundation is based on Geometric Algebra (GA) framework, which enables the representation of harmonic voltages and currents as multidimensional vectors in Euclidean space. The use of the geometric product allows to compute the geometric power multivector. The proposed method is a generalization and extension of previous works that have focused on single-phase and balanced three-phase systems. This paper introduces a complete analysis of new power terms in arbitrary multiphase electrical circuits entirely rooted on Geometric Algebra and Symmetrical Components. Several synthetic and real-world examples are presented to illustrate the novelty, effectiveness and accuracy of the proposed approach. The results of this study contribute to the development of a new geometric foundation for the power theory in electrical engineering.

**Index Terms**—geometric algebra, nonsinusoidal power flow, AC systems, geometric electricity, harmonic power flow

## I. INTRODUCTION

### A. Motivation

The study of power performance in modern AC circuits has gained significant attention due to its vital role in ensuring the safe and efficient distribution of electrical energy within various applications, such as motor driving systems and power electronics. A comprehensive analysis of power characteristics is essential to optimize the operation of these systems, prevent potential instabilities, and ensure their reliability. In recent years, the increasing use of non-linear loads and power electronic devices has led to the presence of harmonics and unbalanced conditions in multiphase AC circuits, complicating the analysis and control of power flow. Traditional methods for analyzing power flow in AC circuits, such as complex numbers and matrices, have limitations when dealing with non-sinusoidal and unbalanced conditions [1]. Moreover, these methods cannot fully capture the interactions between harmonics that occur in such systems. Consequently, power definitions like apparent or reactive power become more intricate [2], [3], resulting in different versions depending on the chosen standard (e.g., IEEE 1459 or DIN 40110). This work aims to address the above-mentioned issues and proposes new tools to study and analyze power flow in non-sinusoidal multiphase circuits in the frequency domain through the powerful framework provided by Geometric Algebra.

### B. Background and Literature Review

The efficient and optimal operation of electrical and power systems has been a topic of interest since the development of apparent and reactive power concepts. Adequate management of these concepts is widely acknowledged as beneficial from both an engineering and economic standpoint. Despite ongoing

debates on the physical interpretation of these concepts, this paper primarily focuses on the economic and optimization aspects of frequency-based power definitions, i.e., how the power definitions affect the optimal operation of power circuits with minimal losses. For an in-depth examination of the physical interpretation of power in this context, readers are referred to [4], [5], [6].

In the context of steady-state analysis, complex numbers and matrix algebra have traditionally been used, along with the Fourier transform in the frequency domain. In the case of multiphase systems, the Fortescue transform (symmetrical components) has proven useful for simplifying the process for unbalanced or asymmetrical systems [7], [8]. However, the interactions between different harmonics and phases involved in the phenomenon of apparent (reactive) power flow cannot be fully addressed using standard mathematical tools such as matrices and complex numbers [9]. Therefore, the role of the mathematical framework is essential in achieving satisfactory results, and this serves as an example of how existing tools are insufficient for the task at hand. In such cases, alternative tools or frameworks should be developed or adapted. For instance, the use of quaternions has shown advantages over matrix algebra in computer vision problems [10] and navigation.

GA has been revealed as a universal and unifying framework that includes a large number of traditional tools such as complex numbers, quaternions, matrices, differential forms, tensors, etc [11]. Recently, its versatility and capability have been demonstrated in various fields of science and engineering such as quantum physics, mechanics, robotics, computer vision, and also electrical engineering [12], [13], [14]. The use of GA makes it possible to solve electrical circuits in both frequency and time domain [15], [16] with a very similar approach. Because of the inherent multidimensionality of electrical systems [17], [18], GA is the appropriate tool to analyze them. For instance, GA makes it possible to compute power flows resulting from the interaction of harmonics of different frequencies, a task that cannot currently be accomplished with complex numbers or matrices [19].

### C. Contributions

This work extends and elaborates on the results of [20] and [21] by presenting the theoretical framework in multiphase electrical circuits using symmetrical components. Specifically, three-phase circuits are thoroughly analyzed in detail. The novel contributions are the following:

- Introducing a new approach for analyzing the power flow in arbitrary multiphase AC circuits from a purely geometric approach using Geometric Algebra framework.
- Generalizing and extending previous works that have focused on single-phase and balanced three-phase circuits to provide a complete analysis of power flow in arbitrary

multiphase non-sinusoidal, non-linear and/or unbalanced electrical circuits.

- Definition of symmetrical components and new power terms resulting from the interaction of current and voltage of different sequences in the GA framework.
- Creation of a comprehensive and unified method to understand harmonic powers in the GA framework.
- Presenting several examples to illustrate the novelty, effectiveness, and accuracy of the proposed approach.
- Contributing to the development of a new geometric foundations for the power theory in electrical engineering.

#### D. Outline

The outline of the paper is as follows. Section II presents a brief overview of the application of geometric algebra to electrical circuits. The concept of isomorphism among vector spaces is crucial to define the voltage and current vector, along with the concept of geometric power multivector. Section III presents the formulation of symmetrical components in the language of GA. The geometric positive, negative and zero sequences are defined using geometric rotors for sinusoidal and non-sinusoidal circuits. A list of scenarios is presented in sections IV and V in increasing order of complexity, from balanced, symmetric and sinusoidal 3-wire systems to asymmetric, non-sinusoidal, unbalanced 4-wire circuits. In Section VI, a practical case is presented highlighting the benefits and advantages of the method for solving complex systems in the real world. Finally, Section VII draws some conclusions.

## II. BRIEF OVERVIEW OF GEOMETRIC ALGEBRA IN ELECTRICAL SYSTEMS

Any periodic electrical signal (voltage or current) can be expressed through the orthonormal basis in the vector space of Fourier functions  $\varphi = \{1, \sqrt{2} \cos k\omega t, \sqrt{2} \sin k\omega t\}_{k=1}^m$ , where  $m$  is the number of harmonics under consideration. This basis is isomorphic [20] to the Euclidean basis  $\sigma = \{\sigma_k\}_{k=0}^{2m}$ , with the following one-to-one mapping

$$\begin{aligned} 1 & \longleftrightarrow \sigma_0 \\ \sqrt{2} \cos \omega t & \longleftrightarrow \sigma_1 \\ \sqrt{2} \sin \omega t & \longleftrightarrow \sigma_2 \\ & \dots \\ \sqrt{2} \cos m\omega t & \longleftrightarrow \sigma_{2m-1} \\ \sqrt{2} \sin m\omega t & \longleftrightarrow \sigma_{2m} \end{aligned} \quad (1)$$

Under this rationale, an arbitrary voltage  $u(t)$  or current  $i(t)$  can be expressed as a vector, denoted by  $\mathbf{u}$  or  $\mathbf{i}$ , respectively. As shown in [20], the geometric product of the voltage and current vectors leads to the geometric power multivector

$$\mathbf{M} = \mathbf{u}\mathbf{i} = \mathbf{u} \cdot \mathbf{i} + \mathbf{u} \wedge \mathbf{i} = P + \mathbf{M}_N \quad (2)$$

where the  $\cdot$  operator means inner/dot product, while  $\wedge$  means exterior/outer product.  $P$  is the well-known active power (scalar value), while  $\mathbf{M}_N$  is the geometric non-active power bivector (see [20], sec. 4). It accounts for the classical reactive power (in the Budeanu sense) but also new terms stemming from the interaction between harmonics of different frequencies. The norm of the geometric power fulfils the pythagorean relationship  $\|\mathbf{M}\|^2 = P^2 + \|\mathbf{M}_N\|^2$ . Moreover, a geometric

impedance bivector  $\mathbf{Z}_k = \mathbf{u}_k \mathbf{i}_k^{-1}$  can be defined for every harmonic  $k$ , with

$$\begin{aligned} \mathbf{u}_k &= u_{2k-1} \sigma_{2k-1} + u_{2k} \sigma_{2k} & u_k &= \sqrt{u_{2k-1}^2 + u_{2k}^2} \\ \mathbf{i}_k &= i_{2k-1} \sigma_{2k-1} + i_{2k} \sigma_{2k} & i_k &= \sqrt{i_{2k-1}^2 + i_{2k}^2} \end{aligned} \quad (3)$$

being  $\mathbf{u}_k$  and  $\mathbf{i}_k$  the vector parts corresponding to harmonic  $k$  for voltage and current, respectively. Thus, the use of GA allows the application of the superposition theorem [15] and, therefore, to solve electrical circuits by applying the well-known laws and theorems of the circuit theory.

## III. SYMMETRICAL COMPONENTS IN GA

### A. Geometric Voltages and Currents

The proposed approach for the analysis of powers in multiphase systems is based on GA and relies on the use of Symmetrical Components (SC) instead of phase values because of the orthogonality and linear independency between sequences. The SC technique involves treating a multiphase system with  $p$  phases as the superposition of  $p$  different and independent balanced systems to compute the currents and the voltage in an easier way. Thus, the complexity of calculations is reduced and simplified. However, this poses a problem for computing powers. For simplicity purposes and due to space limitations, the case of a three-phase ( $p = 3$ ) circuit is presented here, but generalisation to more phases is straightforward (just add more dimensions). The periodic but arbitrary voltages and currents are

$$\begin{aligned} u_p(t) &= \sqrt{2} \sum_{k \in N} U_{pk} \cos(k\omega t + \varphi_{pk}^v) \\ i_p(t) &= \sqrt{2} \sum_{k \in M} I_{pk} \cos(k\omega t + \varphi_{pk}^i) \end{aligned} \quad (4)$$

with  $p = \{R, S, T\}$  the phase numbering,  $k$  integer,  $U_{pk}$ ,  $I_{pk}$  phase RMS values,  $N$  and  $M$  the set of voltage and current harmonics, respectively. DC and interharmonic terms are avoided for simplicity but can be added without loss of generality. Eqs. (4) are transferred to the GA domain as

$$\begin{aligned} \mathbf{u}_p &= \sum_{k \in N} \mathbf{u}_{pk} = \sum_{k \in N} U_{pk} \cos \varphi_{pk}^v \sigma_{2k-1} + U_{pk} \sin \varphi_{pk}^v \sigma_{2k} \\ \mathbf{i}_p &= \sum_{k \in M} \mathbf{i}_{pk} = \sum_{k \in M} I_{pk} \cos \varphi_{pk}^i \sigma_{2k-1} + I_{pk} \sin \varphi_{pk}^i \sigma_{2k} \end{aligned} \quad (5)$$

To facilitate comprehension and streamline the analysis, this paper provides a detailed description of the process, emphasizing the differentiation between sinusoidal and non-sinusoidal scenarios. Moreover, the geometric symmetrical components in power invariant form is applied solely to the voltage vector in Eq. (5) for simplicity.

1) *Sinusoidal case:* For the sinusoidal case, the phase-to-neutral voltage vectors are expressed as

$$\begin{aligned} \mathbf{u}_R &= u_{R1} \sigma_1 + u_{R2} \sigma_2 = u_R e^{\varphi_R \sigma_{12}} \sigma_1 \\ \mathbf{u}_S &= u_{S1} \sigma_1 + u_{S2} \sigma_2 = u_S e^{\varphi_S \sigma_{12}} \sigma_1 \\ \mathbf{u}_T &= u_{T1} \sigma_1 + u_{T2} \sigma_2 = u_T e^{\varphi_T \sigma_{12}} \sigma_1 \end{aligned} \quad (6)$$

Note that the polar form has been used for clarity where the vector  $\mathbf{u}_i$  is expressed as a rotation of the base vector  $\sigma_1$ .

The first step for the geometrical transformation is to compute the geometric sequence voltage vectors as follows

$$\begin{aligned}\bar{\mathbf{u}}_p &= \frac{1}{\sqrt{3}} (\mathbf{u}_R + \mathbf{A}\mathbf{u}_S + \mathbf{A}^\dagger\mathbf{u}_T) \\ \bar{\mathbf{u}}_n &= \frac{1}{\sqrt{3}} (\mathbf{u}_R + \mathbf{A}^\dagger\mathbf{u}_S + \mathbf{A}\mathbf{u}_T) \\ \bar{\mathbf{u}}_0 &= \frac{1}{\sqrt{3}} (\mathbf{u}_R + \mathbf{u}_S + \mathbf{u}_T)\end{aligned}\quad (7)$$

where  $\bar{\mathbf{u}}_p$ ,  $\bar{\mathbf{u}}_n$  and  $\bar{\mathbf{u}}_0$  are the geometric positive, negative and zero sequence vectors, respectively (be aware that the decoration bar has no special meaning). The bivector  $\mathbf{A} = e^{120\sigma_{12}}$  is a *geometric rotor*, performing a  $120^\circ$  rotation in the plane  $\sigma_{12}$  when applied to a vector. The reverse  $\mathbf{A}^\dagger = e^{-120\sigma_{12}}$  also performs a rotation but in the opposite direction. Note that  $\mathbf{A}^2 = \mathbf{A}^\dagger$ , i.e., two consecutive rotations of  $120^\circ$  ( $240^\circ$  in total) in a direction is the same that rotate  $120^\circ$  in the opposite direction. Once the geometric sequence components are obtained, the SC vector is built. For this task, the sequence components must be accommodated in an orthogonal way. The most natural option is to add more dimensions when needed. For the case of 3 sequences, we need 4 extra dimensions, thus the initial basis  $\sigma$  for sinusoidal signals extend from  $\sigma_2$  to  $\sigma_6$ . The proposed method accomplish this task by renumbering the basis vectors for the negative and zero sequences without altering the positive sequence. This will be called the *shifting mechanism* and it reads as follows

$$\begin{aligned}\bar{\mathbf{u}}_p &= u_{p1}\sigma_1 + u_{p2}\sigma_2 \rightarrow \mathbf{u}_p = u_{p1}\sigma_1 + u_{p2}\sigma_2 \\ \bar{\mathbf{u}}_n &= u_{n1}\sigma_1 + u_{n2}\sigma_2 \rightarrow \mathbf{u}_n = u_{n1}\sigma_3 + u_{n2}\sigma_4 \\ \bar{\mathbf{u}}_0 &= u_{01}\sigma_1 + u_{02}\sigma_2 \rightarrow \mathbf{u}_0 = u_{01}\sigma_5 + u_{02}\sigma_6\end{aligned}\quad (8)$$

In this way, the SC voltage vector is simply

$$\begin{aligned}\mathbf{u} &= \mathbf{u}_p + \mathbf{u}_n + \mathbf{u}_0 \\ &= u_{p1}\sigma_1 + u_{p2}\sigma_2 + u_{n1}\sigma_3 + u_{n2}\sigma_4 + u_{01}\sigma_5 + u_{02}\sigma_6\end{aligned}\quad (9)$$

To recover the original signals, the reverse process should be followed, i.e., first split the SC vector into geometric sequence components undoing the shifting process

$$\begin{aligned}\mathbf{u}_p &= u_{p1}\sigma_1 + u_{p2}\sigma_2 \rightarrow \bar{\mathbf{u}}_p = u_{p1}\sigma_1 + u_{p2}\sigma_2 \\ \mathbf{u}_n &= u_{n1}\sigma_3 + u_{n2}\sigma_4 \rightarrow \bar{\mathbf{u}}_n = u_{n1}\sigma_1 + u_{n2}\sigma_2 \\ \mathbf{u}_0 &= u_{01}\sigma_5 + u_{02}\sigma_6 \rightarrow \bar{\mathbf{u}}_0 = u_{01}\sigma_1 + u_{02}\sigma_2\end{aligned}\quad (10)$$

and apply the inverse SC transformation

$$\begin{aligned}\mathbf{u}_R &= \frac{1}{\sqrt{3}} (\bar{\mathbf{u}}_p + \bar{\mathbf{u}}_n + \bar{\mathbf{u}}_0) \\ \mathbf{u}_S &= \frac{1}{\sqrt{3}} (\mathbf{A}^\dagger\bar{\mathbf{u}}_p + \mathbf{A}\bar{\mathbf{u}}_n + \bar{\mathbf{u}}_0) \\ \mathbf{u}_T &= \frac{1}{\sqrt{3}} (\mathbf{A}\bar{\mathbf{u}}_p + \mathbf{A}^\dagger\bar{\mathbf{u}}_n + \bar{\mathbf{u}}_0)\end{aligned}\quad (11)$$

A similar procedure can be carried out for both the sequence and the SC current vectors, resulting in

$$\mathbf{i} = \mathbf{i}_p + \mathbf{i}_n + \mathbf{i}_0\quad (12)$$

Finally, use the isomorphism defined in Eq. (1) to transform the geometric vectors into phase time domain waveforms.

2) *Non-Sinusoidal case*: For the non-sinusoidal case, the method explained in the previous section must be applied for

every harmonic  $k$  present in the electrical phases

$$\begin{aligned}\bar{\mathbf{u}}_{pk} &= \frac{1}{\sqrt{3}} (\mathbf{u}_{Rk} + \mathbf{A}_k\mathbf{u}_{Sk} + \mathbf{A}_k^\dagger\mathbf{u}_{Tk}) \\ \bar{\mathbf{u}}_{nk} &= \frac{1}{\sqrt{3}} (\mathbf{u}_{Rk} + \mathbf{A}_k^\dagger\mathbf{u}_{Sk} + \mathbf{A}_k\mathbf{u}_{Tk}) \\ \bar{\mathbf{u}}_{0k} &= \frac{1}{\sqrt{3}} (\mathbf{u}_{Rk} + \mathbf{u}_{Sk} + \mathbf{u}_{Tk})\end{aligned}\quad (13)$$

where  $\bar{\mathbf{u}}_{pk}$ ,  $\bar{\mathbf{u}}_{nk}$  and  $\bar{\mathbf{u}}_{0k}$  are the positive, negative and zero sequence vectors for harmonic  $k$ , respectively. The bivector  $\mathbf{A}_k = e^{120\sigma_{(2k-1)(2k)}}$  is a geometric rotor performing a  $120^\circ$  rotation in the plane  $\sigma_{(2k-1)(2k)}$ . Note that, in the context of electrical engineering, it is commonly assumed that all sequences exhibit the same type of harmonics  $k$ . Thus, the total positive, negative and zero sequence vectors are

$$\bar{\mathbf{u}}_p = \sum_{i=1}^k \bar{\mathbf{u}}_{pi} \quad \bar{\mathbf{u}}_n = \sum_{i=1}^k \bar{\mathbf{u}}_{ni} \quad \bar{\mathbf{u}}_0 = \sum_{i=1}^k \bar{\mathbf{u}}_{0i}\quad (14)$$

Applying the shifting mechanism, more dimensions will be added depending on the number of harmonics

$$\begin{aligned}\bar{\mathbf{u}}_{pk} &= u_{p1k}\sigma_{2k-1} + u_{p2k}\sigma_{2k} \rightarrow \mathbf{u}_{pk} = u_{p1k}\sigma_{2k-1} + u_{p2k}\sigma_{2k} \\ \bar{\mathbf{u}}_{nk} &= u_{n1k}\sigma_{2k-1} + u_{n2k}\sigma_{2k} \rightarrow \mathbf{u}_{nk} = u_{n1k}\sigma_{4k-1} + u_{n2k}\sigma_{4k} \\ \bar{\mathbf{u}}_{0k} &= u_{01k}\sigma_{2k-1} + u_{02k}\sigma_{2k} \rightarrow \mathbf{u}_{0k} = u_{01k}\sigma_{6k-1} + u_{02k}\sigma_{6k}\end{aligned}\quad (15)$$

Note that the SC vector has now  $6k$  dimensions to accommodate the harmonics of all sequences. It makes sense because it corresponds to the initial number of degrees of freedom of the system. The sequence vectors are then

$$\mathbf{u}_p = \sum_{k=1}^k \mathbf{u}_{pk} \quad \mathbf{u}_n = \sum_{k=1}^k \mathbf{u}_{nk} \quad \mathbf{u}_0 = \sum_{k=1}^k \mathbf{u}_{0k}\quad (16)$$

and the SC vector is

$$\mathbf{u} = \mathbf{u}_p + \mathbf{u}_n + \mathbf{u}_0\quad (17)$$

## B. Geometric Power

Once the sequence vectors and SC vector for voltage and current have been obtained, and according to Eq. (2), the geometric power can be computed as

$$\begin{aligned}\mathbf{M} &= \mathbf{u}\mathbf{i} = (\mathbf{u}_p + \mathbf{u}_n + \mathbf{u}_0)(\mathbf{i}_p + \mathbf{i}_n + \mathbf{i}_0) \\ &= \mathbf{u}_p\mathbf{i}_p + \mathbf{u}_p\mathbf{i}_n + \mathbf{u}_p\mathbf{i}_0 \\ &\quad + \mathbf{u}_n\mathbf{i}_p + \mathbf{u}_n\mathbf{i}_n + \mathbf{u}_n\mathbf{i}_0 \\ &\quad + \mathbf{u}_0\mathbf{i}_p + \mathbf{u}_0\mathbf{i}_n + \mathbf{u}_0\mathbf{i}_0 \\ &= \mathbf{M}_p + \mathbf{M}_n + \mathbf{M}_0 + \mathbf{M}_R = P + \mathbf{M}_N\end{aligned}\quad (18)$$

with

$$\begin{aligned}\mathbf{M}_p &= \mathbf{u}_p\mathbf{i}_p = P^+ + \mathbf{M}_N^+ = P^+ + \mathbf{M}_Q^+ + \mathbf{M}_D^+ \\ \mathbf{M}_n &= \mathbf{u}_n\mathbf{i}_n = P^- + \mathbf{M}_N^- = P^- + \mathbf{M}_Q^- + \mathbf{M}_D^- \\ \mathbf{M}_0 &= \mathbf{u}_0\mathbf{i}_0 = P^0 + \mathbf{M}_N^0 = P^0 + \mathbf{M}_Q^0 + \mathbf{M}_D^0 \\ \mathbf{M}_R &= \mathbf{M} - \mathbf{M}_p - \mathbf{M}_n - \mathbf{M}_0\end{aligned}\quad (19)$$

The terms  $\mathbf{M}_p$ ,  $\mathbf{M}_n$  and  $\mathbf{M}_0$  are the positive, negative and zero sequence geometric power. They are the sum of the positive, negative and zero sequence active power (scalars  $P^+$ ,  $P^-$  and  $P^0$ ) and non-active power (bivectors  $\mathbf{M}_N^+$ ,  $\mathbf{M}_N^-$  and

$M_N^0$ ). The non-active power bivector  $M_N$  can be decomposed into  $M_Q$  which accounts for the geometric reactive power (in the Budeanu sense) and  $M_D$  which accounts for the geometric distorted power, a new power term resulting from the cross-products between voltage and current of different frequencies and same sequence. Finally, bivector  $M_R$  is also a power term due to the interaction of current and voltages of different sequences. This is an original result of this work.

Another distinctive feature (as in the time domain version of this framework [12], [16]) is that the reactive (in the Budeanu sense) power terms  $M_Q$  are grouped into bivectors terms of the form  $\sigma_{(2k-1)(2k)}$  for every harmonic order  $k$ .

#### IV. APPLICATION TO THREE-PHASE SYSTEMS. SINUSOIDAL SUPPLY

In the upcoming sections, the proposed framework will be applied to various three-phase electrical systems taken from the literature and different sources. It will be included both sinusoidal and non-sinusoidal supplies, as well as linear and non-linear loads. The application to sinusoidal sources will first be considered for convenience. This approach aims to provide a comprehensive understanding of the new framework by breaking down the analysis into manageable steps of increasing difficulty. The methodology will be explained in detail, providing examples and applications for each scenario.

##### A. Balanced Load and Symmetric Source 3-wire Circuit

Consider a system with a symmetrical and sinusoidal source and balanced load, where the neutral point can be virtual or real. The phase-to-neutral voltages of the source and the supplied currents are

$$\begin{aligned} u_R(t) &= \sqrt{2}U \cos \omega t & i_R(t) &= \sqrt{2}I \cos(\omega t - \varphi) \\ u_S(t) &= \sqrt{2}U \cos(\omega t - 120) & i_S(t) &= \sqrt{2}I \cos(\omega t - 120 - \varphi) \\ u_T(t) &= \sqrt{2}U \cos(\omega t + 120) & i_T(t) &= \sqrt{2}I \cos(\omega t + 120 - \varphi) \end{aligned}$$

Note that all angles are assumed to be in degrees. The transformation of voltages and currents to the geometrical domain is

$$\begin{aligned} \mathbf{u}_R &= U\sigma_1 & \mathbf{i}_R &= Ie^{-\varphi\sigma_{12}}\sigma_1 \\ \mathbf{u}_S &= UA^\dagger\sigma_1 & \mathbf{i}_S &= IA^\dagger e^{-\varphi\sigma_{12}}\sigma_1 \\ \mathbf{u}_T &= UA\sigma_1 & \mathbf{i}_T &= IAe^{-\varphi\sigma_{12}}\sigma_1 \end{aligned}$$

Again, the polar form has been used for clarity. The geometric SC is now applied to the vectors. Because the system is symmetrical and balanced, we know that there will be no negative or zero sequences in both current and voltage,

$$\begin{aligned} \bar{\mathbf{u}}_p &= \frac{U}{\sqrt{3}} (\sigma_1 + \mathbf{A}\mathbf{A}^\dagger\sigma_1 + \mathbf{A}^\dagger\mathbf{A}\sigma_1) = \sqrt{3}U\sigma_1 \\ \bar{\mathbf{u}}_n &= \frac{U}{\sqrt{3}} (\sigma_1 + \mathbf{A}^\dagger\mathbf{A}^\dagger\sigma_1 + \mathbf{A}\mathbf{A}\sigma_1) = 0 \\ \bar{\mathbf{u}}_0 &= \frac{U}{\sqrt{3}} (\sigma_1 + \mathbf{A}^\dagger\sigma_1 + \mathbf{A}\sigma_1) = 0 \end{aligned} \quad (20)$$

$$\bar{\mathbf{i}}_p = \frac{Ie^{-\varphi\sigma_{12}}}{\sqrt{3}} (\sigma_1 + \mathbf{A}\mathbf{A}^\dagger\sigma_1 + \mathbf{A}^\dagger\mathbf{A}\sigma_1) = \sqrt{3}Ie^{-\varphi\sigma_{12}}\sigma_1$$

$$\bar{\mathbf{i}}_n = \frac{Ie^{-\varphi\sigma_{12}}}{\sqrt{3}} (\sigma_1 + \mathbf{A}^\dagger\mathbf{A}^\dagger\sigma_1 + \mathbf{A}\mathbf{A}\sigma_1) = 0$$

$$\bar{\mathbf{i}}_0 = \frac{Ie^{-\varphi\sigma_{12}}}{\sqrt{3}} (\sigma_1 + \mathbf{A}^\dagger\sigma_1 + \mathbf{A}\sigma_1) = 0 \quad (21)$$

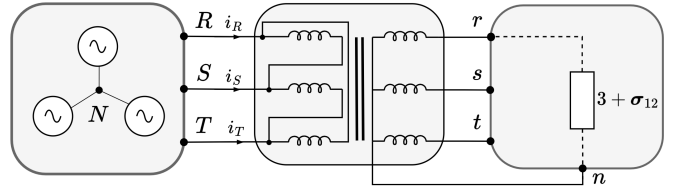


Figure 1: Unbalanced load supplied by a symmetrical voltage source in a 3-wire circuit. The load is composed of a transformer and impedance on the secondary.

where the properties  $\mathbf{A}\mathbf{A}^\dagger = 1$ ,  $(\mathbf{A}^\dagger)^2 = \mathbf{A}$  and  $\mathbf{A}^2 = \mathbf{A}^\dagger$  have been applied. For this simple case, the SC vectors are

$$\begin{aligned} \mathbf{u} &= \mathbf{u}_p = \bar{\mathbf{u}}_p = \sqrt{3}U\sigma_1 & \|\mathbf{u}\| &= \sqrt{3}U \\ \mathbf{i} &= \mathbf{i}_p = \bar{\mathbf{i}}_p = \sqrt{3}Ie^{-\varphi\sigma_{12}}\sigma_1 & \|\mathbf{i}\| &= \sqrt{3}I \end{aligned} \quad (22)$$

The geometric SC power multivector  $\mathbf{M}$  is then computed as

$$\begin{aligned} \mathbf{M} &= \mathbf{u}\mathbf{i} = \sqrt{3}U\sigma_1\sqrt{3}Ie^{-\varphi\sigma_{12}}\sigma_1 \\ &= 3UIe^{\varphi\sigma_{12}} = 3UI \cos \varphi + 3UI \sin \varphi \sigma_{12} \end{aligned} \quad (23)$$

It can be readily checked that  $\|\mathbf{M}\| = \|\mathbf{u}\|\|\mathbf{i}\| = 3UI$ , which coincides with the expected results. Note that the role of the imaginary unit  $j$  in traditional complex phasor computations is now played by the bivector term  $\sigma_{12}$ , since  $\sigma_{12}^2 = -1$ .

##### B. Unbalanced Load and Symmetric Source 3-wire Circuit

The circuit in Fig. 1 represents a symmetrical, sinusoidal system of voltages feeding a highly unbalanced three-phase load. The considered values for the phase-to-neutral voltages at the source are

$$\begin{aligned} u_R(t) &= \sqrt{2}277 \cos(\omega t - 30) \\ u_S(t) &= \sqrt{2}277 \cos(\omega t - 150) \\ u_T(t) &= \sqrt{2}277 \cos(\omega t + 90) \end{aligned}$$

The current can be obtained by the simple application of circuit theory to the set transformer–impedance

$$\begin{aligned} i_R(t) &= \sqrt{2}151.72 \cos(\omega t - 18.43) \\ i_S(t) &= \sqrt{2}151.72 \cos(\omega t + 161.56) \\ i_T(t) &= 0 \end{aligned}$$

The voltages and currents are transformed into the geometric domain as

$$\begin{aligned} \mathbf{u}_R &= 277e^{-30\sigma_{12}}\sigma_1 & \mathbf{i}_R &= 151.72e^{-18.43\sigma_{12}}\sigma_1 \\ \mathbf{u}_S &= 277e^{-150\sigma_{12}}\sigma_1 & \mathbf{i}_S &= 151.72e^{161.56\sigma_{12}}\sigma_1 \\ \mathbf{u}_T &= 277e^{90\sigma_{12}}\sigma_1 & \mathbf{i}_T &= 0 \end{aligned}$$

The sequence components of the voltage and current are now being computed. As in the previous example, it is observed that the voltage is balanced, resulting in the existence of only a positive sequence

$$\bar{\mathbf{u}}_p = \sqrt{3}277e^{-30\sigma_{12}}\sigma_1 \quad (24)$$

In contrast, positive and negative sequences are now present in the current, and thus the basis is now comprised of four base vectors  $\sigma = \{\sigma_1, \sigma_2, \sigma_3, \sigma_4\}$ . Following Eq. (7), the

geometric sequence current vectors are

$$\begin{aligned}\bar{i}_p &= \frac{151.72}{\sqrt{3}} \left( e^{-18.43\sigma_{12}} \sigma_1 + \mathbf{A} e^{161.56\sigma_{12}} \sigma_1 \right) \\ &= 151.72 e^{-48.43\sigma_{12}} \sigma_1 \\ \bar{i}_n &= \frac{151.72}{\sqrt{3}} \left( e^{-18.43\sigma_{12}} \sigma_1 + \mathbf{A}^\dagger e^{161.56\sigma_{12}} \sigma_1 \right) \\ &= 151.72 e^{11.56\sigma_{12}} \sigma_1 \\ \bar{i}_0 &= 0\end{aligned}\quad (25)$$

and based on the shifting mechanism proposed in (8), the shifted sequence vectors are

$$\mathbf{i}_p = 151.72 e^{-48.43\sigma_{12}} \sigma_1 \quad \mathbf{i}_n = 151.72 e^{11.56\sigma_{34}} \sigma_3 \quad (26)$$

The voltage and current SC vectors are then

$$\begin{aligned}\mathbf{u} &= \sqrt{3} 277 e^{-30\sigma_{12}} \sigma_1 \\ \mathbf{i} &= 151.72 e^{-48.43\sigma_{12}} \sigma_1 + 151.72 e^{11.56\sigma_{34}} \sigma_3\end{aligned}$$

The geometric SC power obtained in this particular example is worth

$$\begin{aligned}\mathbf{M} = \mathbf{u}\mathbf{i} &= 69,058 + 23,013\sigma_{12} + 61,760\sigma_{13} \\ &\quad - 12,632\sigma_{14} + 35,657\sigma_{23} - 7293\sigma_{24}\end{aligned}$$

The result will be examined for a moment. As can be observed, there is a scalar value which represents the active power solely caused by the interaction of voltage and current of positive sequence ( $P^+$ ). It is coincident with Joule's law applied to the load  $RI^2 = 3 \cdot 151.72^2 = 69,058$  W. The reactive power  $XI^2 = 1 \cdot 151.72^2 = 23,013$  VAr is represented by the bivector term  $\mathbf{Q} = 23,013\sigma_{12}$ . The interaction between positive sequence voltage and negative sequence current is represented by the remaining bivector terms. The norm of the geometric power is  $|\mathbf{M}| = \sqrt{\langle \mathbf{M}\mathbf{M}^\dagger \rangle_0} = |\mathbf{u}||\mathbf{i}| = 102,943$  VA. One of the advantages of using GA is that the current decomposition can be easily obtained by inverting the voltage vector. In this example, the result is

$$\mathbf{i}_a = \mathbf{u}^{-1}P = \frac{\mathbf{u}}{\|\mathbf{u}\|^2}P = 143.93 e^{-30\sigma_{12}} \sigma_1$$

$$\mathbf{i}_r = \mathbf{u}^{-1}\mathbf{Q}\sigma_{12} = 47.97 e^{-120\sigma_{12}} \sigma_2$$

$$\mathbf{i}_u = \mathbf{i} - \mathbf{i}_a - \mathbf{i}_r = 151.72 e^{11.56\sigma_{34}} \sigma_3$$

Being  $\mathbf{i}_a$ ,  $\mathbf{i}_r$  and  $\mathbf{i}_u$  the geometric active, reactive and unbalanced current, respectively. It can be readily checked that  $\mathbf{i}_a + \mathbf{i}_r + \mathbf{i}_u = \mathbf{i}$ . Note that to recover the time domain signals, Eqs. (9) to (11) must be applied.

### C. Unbalanced Load and Asymmetric Source 3-wire Circuit

The circuit in Fig. 2 represents an asymmetrical, sinusoidal voltage source feeding an unbalanced three-phase load in a 3-wire system. The time domain phase-to-neutral voltages at the source are

$$\begin{aligned}u_R(t) &= \sqrt{2} 100 \cos \omega t \\ u_S(t) &= \sqrt{2} 100 \cos(\omega t - 120) \\ u_T(t) &= 0\end{aligned}$$

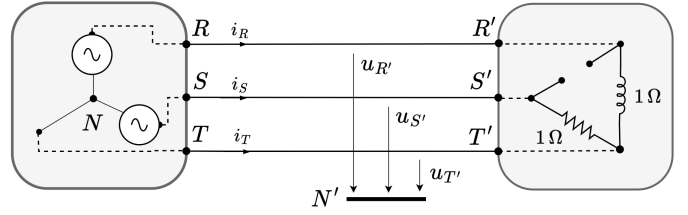


Figure 2: Unbalanced load supplied by an asymmetrical sinusoidal voltage source in a 3-wire circuit.

The line voltages can be readily derived and jointly transformed to the geometric domain as

$$\begin{aligned}u_R &= 100\sigma_1 & u_{RS} &= \sqrt{3} 100 e^{30\sigma_{12}} \sigma_1 \\ u_S &= 100 e^{-120\sigma_{12}} \sigma_1 & u_{ST} &= 100 e^{-120\sigma_{12}} \sigma_1 \\ u_T &= 0 & u_{TR} &= -100\sigma_1\end{aligned}$$

The configuration of the load is that of an unbalanced delta so that solving for the currents, one gets

$$\begin{aligned}i_R(t) &= \sqrt{2} 100 \cos(\omega t - 90) \\ i_S(t) &= \sqrt{2} 100 \cos(\omega t - 120) \\ i_T(t) &= \sqrt{2} 193.18 \cos(\omega t + 75)\end{aligned}$$

The geometrical counterpart is computed as usual

$$\begin{aligned}\mathbf{i}_R &= 100\sigma_2 \\ \mathbf{i}_S &= 100 e^{-120\sigma_{12}} \sigma_1 \\ \mathbf{i}_T &= 193.18 e^{75\sigma_{12}} \sigma_1\end{aligned}$$

The next step is to compute the sequence components of the voltage source

$$\begin{aligned}\bar{u}_p &= \frac{100}{\sqrt{3}} (\sigma_1 + \mathbf{A}\mathbf{A}^\dagger \sigma_1) = \frac{200}{\sqrt{3}} \sigma_1 \\ \bar{u}_n &= \frac{100}{\sqrt{3}} (\sigma_1 + \mathbf{A}^\dagger \mathbf{A}^\dagger \sigma_1) = \frac{100}{\sqrt{3}} e^{60\sigma_{12}} \sigma_1 \\ \bar{u}_0 &= \frac{100}{\sqrt{3}} (\sigma_1 + \mathbf{A}^\dagger \sigma_1) = \frac{100}{\sqrt{3}} e^{-60\sigma_{12}} \sigma_1\end{aligned}$$

Since the load has no neutral and it is unbalanced, a neutral displacement  $\mathbf{u}_{NN'}$  will occur. Therefore, this means that the phase voltages at the load do not match the phase voltages at the source. To compute these phase voltages at the load, the zero sequence is removed and the SC method is applied

$$\begin{aligned}u_{R'} &= \frac{1}{\sqrt{3}} (\bar{u}_p + \bar{u}_n) = \frac{1}{\sqrt{3}} \left( \frac{200}{\sqrt{3}} \sigma_1 + \frac{100}{\sqrt{3}} e^{60\sigma_{12}} \sigma_1 \right) \\ &= 88.19 e^{19.1\sigma_{12}} \sigma_1 \\ u_{S'} &= \frac{1}{\sqrt{3}} (\mathbf{A}^\dagger \bar{u}_p + \mathbf{A} \bar{u}_n) \\ &= \frac{1}{\sqrt{3}} \left( \mathbf{A}^\dagger \frac{200}{\sqrt{3}} \sigma_1 + \mathbf{A} \frac{100}{\sqrt{3}} e^{60\sigma_{12}} \sigma_1 \right) \\ &= 88.19 e^{-139.1\sigma_{12}} \sigma_1 \\ u_{T'} &= \frac{1}{\sqrt{3}} (\mathbf{A} \bar{u}_p + \mathbf{A}^\dagger \bar{u}_n) \\ &= \frac{1}{\sqrt{3}} \left( \mathbf{A} \frac{200}{\sqrt{3}} \sigma_1 + \mathbf{A}^\dagger \frac{100}{\sqrt{3}} e^{60\sigma_{12}} \sigma_1 \right) \\ &= 33.33 e^{120\sigma_{12}} \sigma_1\end{aligned}$$

Note that no zero sequence component should be present at the load because of the 3-wire configuration. Now, the sequence currents are computed

$$\begin{aligned}\bar{i}_p &= \frac{1}{\sqrt{3}} (100\sigma_2 + \mathbf{A}100e^{-120\sigma_{12}}\sigma_1 + \mathbf{A}^\dagger 193.18e^{75\sigma_{12}}\sigma_1) \\ &= 193.18e^{-45\sigma_{12}}\sigma_1\end{aligned}$$

$$\begin{aligned}\bar{i}_n &= \frac{1}{\sqrt{3}} (100\sigma_2 + \mathbf{A}^\dagger 100e^{-120\sigma_{12}}\sigma_1 + \mathbf{A}193.18e^{75\sigma_{12}}\sigma_1) \\ &= \sqrt{2}100e^{-165\sigma_{12}}\sigma_1\end{aligned}$$

$$\bar{i}_0 = 0 \quad (27)$$

The final step involves the computation of the shifted sequence and SC vectors. Note that now the basis has 4 elements from  $\sigma_1$  to  $\sigma_4$  to accommodate the two non-null sequences in the voltage at the load. The SC voltage and current vectors are

$$\begin{aligned}\mathbf{u} &= \frac{200}{\sqrt{3}}\sigma_1 + \frac{100}{\sqrt{3}}e^{60\sigma_{34}}\sigma_3 \\ \mathbf{i} &= 193.18e^{-45\sigma_{12}}\sigma_1 + \sqrt{2}100e^{-165\sigma_{34}}\sigma_3\end{aligned}$$

and the geometric power is

$$\begin{aligned}\mathbf{M} = \mathbf{u}\mathbf{i} &= 10,000 + 15,773\sigma_{12} - 19,716\sigma_{13} + 11,056\sigma_{14} \\ &\quad - 3943\sigma_{23} + 6829\sigma_{24} - 5773\sigma_{34}\end{aligned}$$

Notice that the total active power is the sum of the positive and negative sequence active power  $P = P^+ + P^- = 15,773 - 5773 = 10,000$  W. Furthermore, it corresponds to the total expected active power  $RI_S^2 = 10,000$  W. The traditional reactive power  $XI_S^2 = 10,000$  VAR is disaggregated into the bivector terms  $15,773\sigma_{12}$  and  $-5773\sigma_{34}$  corresponding to the reactive power of the positive and negative sequence, respectively. The decomposition of currents is as follows

$$\mathbf{i} = \mathbf{u}^{-1}\mathbf{M} = \frac{\mathbf{u}}{\|\mathbf{u}\|^2}(P + M_N) = \mathbf{i}_a + \mathbf{i}_N$$

where  $\mathbf{i}_a$  is the geometrical active current (similar to that of the traditional Fryze decomposition) and  $\mathbf{i}_N$  is the non-active current. A typical compensator would take care of removing the non-active component of the current so that the minimum possible current is obtained from the supply grid. Nonetheless, this step may not be optimal as negative sequence components, which can be harmful to the electrical equipment, would still exist. An alternative approach could be to compensate for a fully sinusoidal current consisting solely of positive sequence components demanding the same active power  $P^+ = 15,773$  W, then

$$\mathbf{i}^+ = \mathbf{u}_p^{-1}P^+ = 136.6\sigma_1$$

so that the current to be generated by the active compensator will be  $\mathbf{i}_{\text{comp}} = \mathbf{i} - \mathbf{i}^+$ . Obviously, the negative sequence component of the voltage must be removed as a preliminary step. Otherwise, the active power and the resulting current will be lower since  $\|\mathbf{u}\| > \|\mathbf{u}_p\|$ . In general, it is possible to establish different compensation policies depending on the practical interest of each application.

#### D. Unbalanced Load and Symmetric Source 4-wire Circuit

The attention is now shifted towards three-phase 4-wire circuits, wherein distinct configurations will be examined. The balanced load with symmetrical power supply configuration

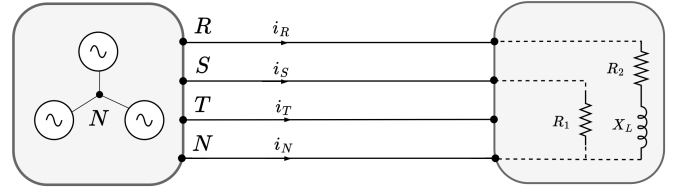


Figure 3: Unbalanced load supplied by a symmetrical sinusoidal voltage source in a 4-wire circuit. The values for the load are  $R_1 = R_2 = 0.5 \Omega$  and  $X_L = 0.87 \Omega$ .

is skipped as it is solved in the same way as a 3-wire system because there is no zero sequence component. A three-phase 4-wire circuit with symmetrical sinusoidal supply and unbalanced load is shown in Fig. 3. The phase-to-neutral voltage supply is given by

$$\begin{aligned}u_R(t) &= \sqrt{2}120 \cos \omega t \\ u_S(t) &= \sqrt{2}120 \cos(\omega t - 120) \\ u_T(t) &= \sqrt{2}120 \cos(\omega t + 120)\end{aligned}$$

with transformed voltages to the geometric domain as

$$\begin{aligned}\mathbf{u}_R &= 120\sigma_1 \\ \mathbf{u}_S &= 120e^{-120\sigma_{12}}\sigma_1 \\ \mathbf{u}_T &= 120e^{120\sigma_{12}}\sigma_1\end{aligned}$$

Since it is a symmetrical power supply, there is only a positive sequence component with value  $\bar{\mathbf{u}}_p = \sqrt{3}120\sigma_1$ . Solving the circuit for the impedances  $\mathbf{Z}_{RN} = 0.5 + 0.87\sigma_{12}$  and  $\mathbf{Z}_{SN} = 0.5$ , the following currents are obtained

$$\begin{aligned}\mathbf{i}_R &= 119.59e^{-60.11\sigma_{12}}\sigma_1 & \mathbf{i}_T &= 0 \\ \mathbf{i}_S &= 240e^{-120\sigma_{12}}\sigma_1 & \mathbf{i}_N &= 317.33e^{79.02\sigma_{12}}\sigma_1\end{aligned}$$

After the computation of the sequence vectors and taking into account the shifting process, the shifted sequence components of the current are worth

$$\begin{aligned}\mathbf{i}_p &= 172.97\sigma_1 + 59.86\sigma_2 = 183.03e^{-19.09\sigma_{12}}\sigma_1 \\ \mathbf{i}_n &= -34.88\sigma_3 - 60.14\sigma_4 = 69.52e^{120.11\sigma_{34}}\sigma_3 \\ \mathbf{i}_0 &= -34.88\sigma_5 + 179.86\sigma_6 = 183.21e^{-100.97\sigma_{56}}\sigma_5\end{aligned} \quad (28)$$

The geometric SC vectors are

$$\begin{aligned}\mathbf{u} &= \sqrt{3}120\sigma_1 \\ \mathbf{i} &= 183.03e^{-19.09\sigma_{12}}\sigma_1 + 69.52e^{120.11\sigma_{34}}\sigma_3 \\ &\quad + 183.21e^{-100.97\sigma_{56}}\sigma_5\end{aligned}$$

The result for the geometric power follows

$$\begin{aligned}\mathbf{M} = \mathbf{u}\mathbf{i} &= 35,950.66 + 12,442.14\sigma_{12} - 7249.34\sigma_{13} \\ &\quad - 12,499.39\sigma_{14} - 7249.34\sigma_{15} + 37,383.68\sigma_{16}\end{aligned}$$

In this example, it can be recognised that there are different bivector terms resulting from the interaction of the positive voltage sequence and the negative and zero current sequences. The expected active power value according to Joule's law is

$$R_1 I_R^2 + R_2 I_S^2 = 0.5 \cdot 119.59^2 + 0.5 \cdot 240^2 = 35,950.66 \text{ W}$$

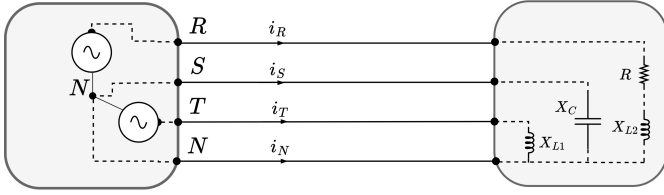


Figure 4: Unbalanced load supplied by an asymmetrical sinusoidal voltage source in a 4-wire circuit. The values for the load are  $R = 1 \Omega$ ,  $X_{L1} = 0.5 \Omega$ ,  $X_{L2} = 1 \Omega$  and  $X_C = 1 \Omega$ .

and the reactive power according to Budeanu is

$$X_2 I_R^2 = 0.87 \cdot 119.59^2 = 12,442.14 \text{ VAR}$$

### E. Unbalanced Load and Asymmetric Source 4-wire Circuit

Adding further complexity to the circuit structure, an unbalanced 4-wire circuit with an asymmetrical sinusoidal supply is shown in Fig. 4. The values of the phase-to-neutral voltages are

$$\begin{aligned} u_R(t) &= \sqrt{2} 100 \cos \omega t \\ u_S(t) &= 0 \\ u_T(t) &= \sqrt{2} 100 \cos(\omega t + 120) \end{aligned}$$

with transformed values to the geometrical domain as

$$\mathbf{u}_R = 100\sigma_1 \quad \mathbf{u}_S = 0 \quad \mathbf{u}_T = 100e^{120}\sigma_{12}\sigma_1$$

Solving the circuit for the impedances specified in Fig. 4, the currents in the geometrical domain are obtained

$$\begin{aligned} \mathbf{i}_R &= 50\sigma_1 + 50\sigma_2 & \mathbf{i}_T &= 173.2\sigma_1 - 100\sigma_2 \\ \mathbf{i}_S &= 0 & \mathbf{i}_N &= -223.2\sigma_1 + 50\sigma_2 \end{aligned}$$

In this case, the rectangular form has been chosen instead of the polar form, in no order of preference. The geometric shifted sequence vectors are

$$\begin{aligned} \mathbf{u}_p &= 115.47\sigma_1 & \mathbf{i}_p &= 28.86\sigma_1 + 144.3376\sigma_2 \\ \mathbf{u}_n &= 28.86\sigma_3 + 50\sigma_4 & \mathbf{i}_n &= -71.13\sigma_3 - 28.86\sigma_4 \\ \mathbf{u}_0 &= 28.86\sigma_5 - 50\sigma_6 & \mathbf{i}_0 &= 128.86\sigma_5 - 28.86\sigma_6 \end{aligned}$$

and the SC vectors are

$$\begin{aligned} \mathbf{u} &= 115.47\sigma_1 + 28.86\sigma_3 + 50\sigma_4 + 28.86\sigma_5 - 50\sigma_6 \\ \mathbf{i} &= 28.86\sigma_1 + 144.33\sigma_2 - 71.13\sigma_3 - 28.86\sigma_4 \\ &\quad + 128.86\sigma_5 - 28.86\sigma_6 \end{aligned}$$

Computing again the geometric power, we get

$$\begin{aligned} \mathbf{M} = \mathbf{u}\mathbf{i} &= 5000 + 16,666.66\sigma_{12} + 2723.29\sigma_{34} \\ &\quad + 5610.04\sigma_{56} + \mathbf{R} \end{aligned}$$

where the term  $\mathbf{R}$  represents the bivector terms due to the interaction between different sequences. Once again, Joule's law is fulfilled and the reactive power due to the positive, negative and zero sequences is accommodated into bivector terms  $\sigma_{12}$ ,  $\sigma_{34}$  and  $\sigma_{56}$ , respectively. The magnitude of the geometric power is  $\|\mathbf{M}\| = \|\mathbf{u}\|\|\mathbf{i}\| = 30,000 \text{ VA}$ . It can be readily checked that the Pythagorean relationship is also fulfilled because of the inherent orthogonality among the terms in the multivector  $\mathbf{M}$ . The geometric power factor is defined as

$$pf = \frac{P}{\|\mathbf{M}\|} = 0.1667$$

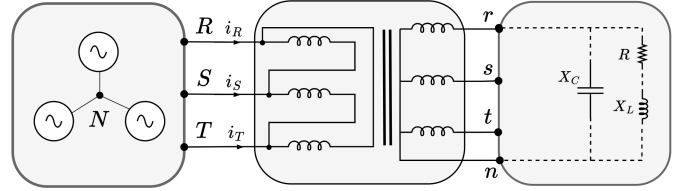


Figure 5: Unbalanced load supplied by a symmetrical non-sinusoidal voltage source in a 3-wire circuit. The values for the load are  $R = 1 \Omega$ ,  $X_L = 2 \Omega$  and  $X_C = 2.5 \Omega$ . The transformer ratio is 1:1.

## V. APPLICATION TO THREE-PHASE SYSTEMS. NON-SINUSOIDAL SUPPLY

In this section, the method is applied to systems supplied by non-sinusoidal sources, thus generating steady-state harmonics. As in the previous sections, different scenarios with an increasing level of complexity are considered.

### A. Unbalanced Load and Symmetric Source 3-wire Circuit

Henceforth, non-sinusoidal circuits will be considered in detail. They present a greater analytical challenge due to harmonic distortions. Figure 5 depicts a system where a symmetrical, non-sinusoidal voltage supplies an unbalanced three-phase load. This configuration is analogous to others studied previously, with the exception that the negative sequence component is conveyed by a negative sequence harmonic, rather than a source asymmetry. As will be demonstrated, the resolution methodology is similar.

The values of the phase-to-neutral voltages are

$$\begin{aligned} u_R(t) &= \sqrt{2} 277 \cos \omega t + \sqrt{2} 11 \cos(5\omega t) \\ u_S(t) &= \sqrt{2} 277 \cos(\omega t - 120) + \sqrt{2} 11 \cos(5\omega t + 120) \\ u_T(t) &= \sqrt{2} 277 \cos(\omega t + 120) + \sqrt{2} 11 \cos(5\omega t - 120) \end{aligned}$$

It is noteworthy that the fifth-order harmonic is characterized by a negative sequence. Consequently, to account for the involvement of two harmonics, a 4-dimensional basis is necessary to conform to the geometric domain

$$\begin{aligned} \sqrt{2} \cos \omega t &\rightarrow \sigma_1 & \sqrt{2} \cos 5\omega t &\rightarrow \sigma_3 \\ \sqrt{2} \sin \omega t &\rightarrow \sigma_2 & \sqrt{2} \sin 5\omega t &\rightarrow \sigma_4 \end{aligned}$$

The geometric voltage vectors are now

$$\begin{aligned} \mathbf{u}_R &= 277\sigma_1 + 11\sigma_3 \\ \mathbf{u}_S &= 277e^{-120}\sigma_{12}\sigma_1 + 11e^{120}\sigma_{34}\sigma_3 \\ \mathbf{u}_T &= 277e^{120}\sigma_{12}\sigma_1 + 11e^{-120}\sigma_{34}\sigma_3 \end{aligned}$$

The load configuration is unbalanced, with only phase R in the secondary circuit being loaded. As a result, the currents are

$$\begin{aligned} i_R(t) &= \sqrt{2} 95.95 \cos(\omega t + 30) + \sqrt{2} 36.2 \cos(5\omega t + 59.702) \\ i_S(t) &= \sqrt{2} 95.95 \cos(\omega t - 150) + \sqrt{2} 36.2 \cos(5\omega t - 120.298) \\ i_T(t) &= 0 \end{aligned}$$

The geometric transformation for the currents is

$$\begin{aligned} \mathbf{i}_R &= 95.95e^{30}\sigma_{12}\sigma_1 + 36.2e^{59.70158}\sigma_{34}\sigma_3 \\ \mathbf{i}_S &= 95.95e^{-150}\sigma_{12}\sigma_1 + 36.2e^{-120.298}\sigma_{34}\sigma_3 \\ \mathbf{i}_T &= 0 \end{aligned}$$

Hence, the determination of symmetrical components at the source is now feasible. Given the presence of two harmonics, the calculation of sequences requires their separate evaluation

$$\begin{aligned} \bar{u}_{p1} &= \sqrt{3}277\sigma_1 & \bar{u}_{n1} &= 0 & \bar{u}_{01} &= 0 \\ \bar{u}_{p5} &= 0 & \bar{u}_{n5} &= \sqrt{3}11\sigma_3 & \bar{u}_{05} &= 0 \end{aligned}$$

The SC for the current is worth

$$\begin{aligned} \bar{i}_{p1} &= 95.95\sigma_1 & \bar{i}_{n1} &= 95.95e^{60\sigma_{12}}\sigma_1 & \bar{i}_{01} &= 0 \\ \bar{i}_{p5} &= 36.22e^{29.7\sigma_{34}}\sigma_3 & \bar{i}_{n5} &= 36.22e^{89.7\sigma_{34}}\sigma_3 & \bar{i}_{05} &= 0 \end{aligned}$$

To obtain the sequence shifted vectors, it is necessary to consider the expressions given in Eqs. (13) through (16). In this particular case, the dimensionality of the problem is  $n = 8$  as a result of the presence of two harmonics and two sequences (positive and negative). The following table presents a summary of the mapping:

positive seq.	negative seq.	
$\sqrt{2} \cos \omega t \rightarrow \sigma_1$	$\sqrt{2} \cos \omega t \rightarrow \sigma_5$	(29)
$\sqrt{2} \sin \omega t \rightarrow \sigma_2$	$\sqrt{2} \sin \omega t \rightarrow \sigma_6$	
$\sqrt{2} \cos 5\omega t \rightarrow \sigma_3$	$\sqrt{2} \cos 5\omega t \rightarrow \sigma_7$	
$\sqrt{2} \sin 5\omega t \rightarrow \sigma_4$	$\sqrt{2} \sin 5\omega t \rightarrow \sigma_8$	

Therefore, the geometrical voltage and current are now expressed as

$$\begin{aligned} \mathbf{u} &= \sqrt{3}277\sigma_1 + \sqrt{3}11\sigma_7 \\ \mathbf{i} &= 95.95\sigma_1 + 36.22e^{29.7\sigma_{34}}\sigma_3 + 95.95e^{60\sigma_{56}}\sigma_5 \\ &\quad + 36.22e^{89.7\sigma_{78}}\sigma_7 \end{aligned}$$

which yields the geometric power

$$\begin{aligned} \mathbf{M} = \mathbf{u}\mathbf{i} &= \underbrace{46,037}_{P^+} + \underbrace{3.1}_{P^-} + 15,094\sigma_{13} - 8609\sigma_{14} \\ &+ 23,018\sigma_{15} - 39,869\sigma_{16} - 1737\sigma_{17} - 17,377\sigma_{18} \\ &- 599\sigma_{37} + 341\sigma_{47} - 914\sigma_{57} + 1583\sigma_{67} - \underbrace{690.07}_{Q^-}\sigma_{78} \end{aligned}$$

Different components with engineering significance can be identified. The geometric power has two components, a scalar and a bivector. The scalar part includes the active power components  $P = P^+ + P^-$ . The negative sequence reactive power  $Q = Q^-$  is accommodated in the bivector  $\sigma_{78}$ . The remaining bivectors account for the interactions between harmonics of different frequencies and/or sequences. In this scenario, the reactive power is exclusively attributed to the fifth harmonic, given that there is no phase shift between the positive sequence voltage and current for the fundamental component. It is noteworthy that these spurious powers, which arise from cross-interactions between sequences and/or harmonics, are not addressed by conventional methods that rely on complex numbers and matrices. The magnitude of the current and voltage vectors and power multivector is shown below

$$\begin{aligned} \|\mathbf{u}\| &= \sqrt{3(277^2 + 11^2)} = 480.15 \text{ V} \\ \|\mathbf{i}\| &= \sqrt{95.95^2 + 36.22^2 + 95.95^2 + 36.22^2} = 145.04 \text{ A} \\ \|\mathbf{M}\| &= \sqrt{\langle \mathbf{M}\mathbf{M}^\dagger \rangle_0} = \|\mathbf{u}\|\|\mathbf{i}\| = 69,645 \text{ VA} \end{aligned} \quad (30)$$

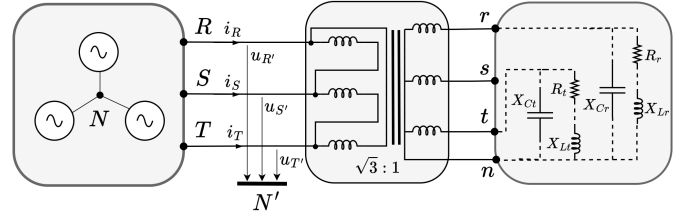


Figure 6: Unbalanced load supplied by an asymmetrical non-sinusoidal voltage source in a 3-wire circuit.

	$\sigma_1$	$\sigma_2$	$\sigma_3$	$\sigma_4$	$\sigma_5$	$\sigma_6$	$\sigma_7$	$\sigma_8$	$\ \cdot\ $
$u_R$	100.00	0.00	30.00	0.00	20.00	0.00	10.00	0.00	106.77
$u_S$	-50.00	86.60	30.00	0.00	-10.00	-17.32	-5.00	8.66	106.77
$u_T$	-25.00	-43.30	15.00	0.00	-5.00	8.66	-2.50	-4.33	53.38
$\bar{u}_p$	144.33	0.00	4.33	-7.50	2.88	5.00	14.43	0.00	145.43
$\bar{u}_n$	14.43	-25.00	4.33	7.50	28.87	0.00	1.44	-2.50	41.83
$\bar{u}_0$	14.43	25.00	43.30	0.00	2.89	-5.00	1.44	2.50	52.44
$u_R$	91.66	-14.43	5.00	0.00	18.33	2.88	9.16	-1.44	95.22
$u_S$	-58.33	72.17	5.00	0.00	-11.67	-14.43	5.83	7.22	95.22
$u_T$	-33.33	-57.73	-10.00	0.00	-6.67	11.55	-3.33	-5.77	69.04
$u_{RS}$	150.00	-86.60	0.00	0.00	30.00	17.32	15.00	-8.66	177.48
$u_{ST}$	-25.00	129.90	15.00	0.00	-5.00	-25.98	-2.50	12.99	136.38
$u_{TR}$	-125.00	-43.30	-15.00	0.00	-25.00	8.66	-12.50	-4.33	136.38

Table I: Phase and sequence geometric voltages for circuit in Fig. 6. All values in volts [V].

### B. Unbalanced Load and Asymmetrical Source 3-wire Circuit

Consider the circuit depicted in Fig. 6, where a non-sinusoidal, asymmetrical power supply is delivering energy to an unbalanced 3-wire load. The value for the phase-to-neutral voltage in phase R is

$$u_R(t) = \sqrt{2}(100 \cos \omega t + 30 \cos 3\omega t + 20 \cos 5\omega t + 10 \cos 7\omega t)$$

The voltage for the phase-to-neutral S and T is worth  $u_S(t) = u_R(t - T/3)$  y  $u_T(t) = 0.5u_R(t + T/3)$ , respectively. The impedances connected to the secondary of the transformer have the following values

$$R_R = X_R = R_T = X_T = 1 \Omega \quad B_R = B_T = 0.5 \text{ S}$$

Harmonics of different sequences are evidenced in the voltage. Furthermore, it is worth noting that line S is not loaded, which results in an unbalanced configuration of the overall system. Following the proposed methodology, the initial step involves transforming the phase voltages and line currents into the geometric domain, followed by the computation of the shifted sequence components, and ultimately the construction of the SC voltage and current vector. As the load in the current system is unbalanced, there will be neutral displacement between the source and load, causing the zero sequence component in the primary of the transformer to be null. In this case, the selected basis has a dimensionality of  $k = s \times (2n) = 16$ , with  $n = 4$  representing the number of harmonics and  $s = 2$  the two non-null sequences (positive and negative). Table I lists the phase voltages at the source and load, line voltages, and symmetrical components in the geometric domain. The line currents are obtained by solving the circuit using KCL, and their values in the geometric domain, as well as the symmetrical components, are presented in Table II.

The construction of the SC voltage and current vector is the final step following the proposed method. This involves combining the results of the sequence components, taking

	$\sigma_1$	$\sigma_2$	$\sigma_3$	$\sigma_4$	$\sigma_5$	$\sigma_6$	$\sigma_7$	$\sigma_8$	$\ \cdot\ $
$i_R$	137.50	-21.65	1.50	-18.00	22.08	-126.47	-14.01	-92.54	212.00
$i_S$	-75.00	43.30	0.00	0.00	-41.09	68.50	28.82	50.60	131.42
$i_T$	-62.50	-21.65	-1.50	18.00	19.00	57.97	-14.81	41.94	102.00
$\tilde{i}_p$	151.55	-12.50	-7.70	-16.34	24.39	-79.48	-7.80	-101.95	202.04
$\tilde{i}_n$	86.60	-25.00	10.30	-14.84	13.86	-139.57	-16.46	-58.33	178.31

Table II: Line and sequence geometric currents in Fig. 6. All values in amperes [A].

	#1	#3	#5	#7	Total
$P_+$	21,875.00	89.19	-327.00	-112.57	21,524.63
$P_-$	1875.22	-66.69	400.15	122.07	2330.52
$P$	23,750.22	22.50	73.15	9.50	<b>23,855.15</b>
$Q_+$	-1804.22	-128.50	-351.40	-1471.60	-3755.70
$Q_-$	1804.22	-141.50	-4029.07	-125.35	-2491.70
$Q$	0.00	-270.00	-4380.45	-1596.95	<b>-6247.40</b>

Table III: Active and reactive harmonic power decomposition for the circuit in Fig. 6. Units of  $P$  in Watts and  $Q$  in VAR.

into account that there are only two sequences. The base is constructed in the same way as in (29)

$$\begin{aligned} \mathbf{u} = & 144.33\sigma_1 + 4.33\sigma_3 - 7.5\sigma_4 + 2.88\sigma_5 + 5\sigma_6 \\ & + 14.43\sigma_7 + 14.43\sigma_9 - 25\sigma_{10} + 4.33\sigma_{11} + 7.5\sigma_{12} \\ & + 28.87\sigma_{13} + 1.44\sigma_{15} - 2.50\sigma_{16} \end{aligned}$$

$$\begin{aligned} \mathbf{i} = & 151.55\sigma_1 - 12.5\sigma_2 - 7.70\sigma_3 - 16.34\sigma_4 + 24.39\sigma_5 \\ & - 79.48\sigma_6 - 7.8\sigma_7 - 101.95\sigma_8 + 86.6\sigma_9 - 25\sigma_{10} + 10.3\sigma_{11} \\ & - 14.84\sigma_{12} + 13.86\sigma_{13} - 139.57\sigma_{14} - 16.46\sigma_{15} - 58.33\sigma_{16} \end{aligned}$$

Now, the product can be performed to obtain the geometrical power. Naturally, due to the high number of harmonics, numerous non-active power cross terms will appear. The most interesting power values, including active and reactive power, are summarised in the Table III. The decomposition of currents could be done as explained previously so that the minimum current (in the Fryze sense) can be found, or unwanted harmonic and negative sequence components can be eliminated.

### C. Unbalanced Load and Symmetric Source 4-wire Circuit

The circuit shown in Fig. 7, illustrates a 4-wire unbalanced system with a symmetrical non-sinusoidal power supply. It includes harmonic components with RMS values are  $U_1 = 240$  V,  $U_3 = 4.8$  V,  $U_5 = 7.2$  V and  $U_7 = 3.6$  V. The values of the admittances for each harmonic are  $\mathbf{Y}_1 = 0.5$ ,  $\mathbf{Y}_3 = 0.1 + 1.2\sigma_{34}$ ,  $\mathbf{Y}_5 = 0.038 + 2.31\sigma_{56}$  and  $\mathbf{Y}_7 = 0.02 + 3.36\sigma_{78}$ . Following the same methodology as in section V-A, the symmetrical components for each voltage and current harmonic

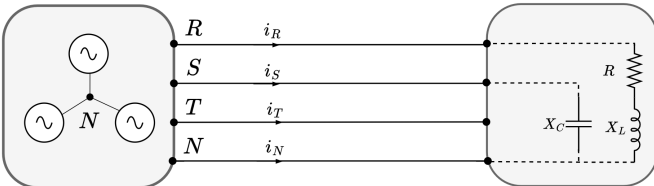


Figure 7: Unbalanced load supplied by a symmetrical non-sinusoidal voltage source in a 4-wire circuit.

	positive	negative	zero
#1	$\sqrt{2} \cos \omega t \rightarrow \sigma_1$	$\sqrt{2} \cos \omega t \rightarrow \sigma_9$	$\sqrt{2} \cos \omega t \rightarrow \sigma_{17}$
	$\sqrt{2} \sin \omega t \rightarrow \sigma_2$	$\sqrt{2} \sin \omega t \rightarrow \sigma_{10}$	$\sqrt{2} \sin \omega t \rightarrow \sigma_{18}$
#3	$\sqrt{2} \cos 3\omega t \rightarrow \sigma_3$	$\sqrt{2} \cos 3\omega t \rightarrow \sigma_{11}$	$\sqrt{2} \cos 3\omega t \rightarrow \sigma_{19}$
	$\sqrt{2} \sin 3\omega t \rightarrow \sigma_4$	$\sqrt{2} \sin 3\omega t \rightarrow \sigma_{12}$	$\sqrt{2} \sin 3\omega t \rightarrow \sigma_{20}$
#5	$\sqrt{2} \cos 5\omega t \rightarrow \sigma_5$	$\sqrt{2} \cos 5\omega t \rightarrow \sigma_{13}$	$\sqrt{2} \cos 5\omega t \rightarrow \sigma_{21}$
	$\sqrt{2} \sin 5\omega t \rightarrow \sigma_6$	$\sqrt{2} \sin 5\omega t \rightarrow \sigma_{14}$	$\sqrt{2} \sin 5\omega t \rightarrow \sigma_{22}$
#7	$\sqrt{2} \cos 7\omega t \rightarrow \sigma_7$	$\sqrt{2} \cos 7\omega t \rightarrow \sigma_{15}$	$\sqrt{2} \cos 7\omega t \rightarrow \sigma_{23}$
	$\sqrt{2} \sin 7\omega t \rightarrow \sigma_8$	$\sqrt{2} \sin 7\omega t \rightarrow \sigma_{16}$	$\sqrt{2} \sin 7\omega t \rightarrow \sigma_{24}$

Table IV: Mapping of Fourier base and Euclidean base for the circuit in Fig. 7.

	#1		#3		#5		#7		$\ \cdot\ $
	$\sigma_1$	$\sigma_2$	$\sigma_3$	$\sigma_4$	$\sigma_5$	$\sigma_6$	$\sigma_7$	$\sigma_8$	
$u_R$	240.00	0.00	4.80	0.00	7.20	0.00	3.60	0.00	240.18
$u_S$	-120.00	207.85	4.80	0.00	-3.60	-6.23	-1.80	3.12	240.18
$u_T$	-120.00	-207.85	4.80	0.00	-3.60	6.23	-1.80	-3.12	240.18
$\tilde{u}_p$	415.69	0.00	0.00	0.00	0.00	0.00	6.24	0.00	415.74
$\tilde{u}_n$	0.00	0.00	0.00	0.00	12.47	0.00	0.00	0.00	12.47
$\tilde{u}_0$	0.00	0.00	8.31	0.00	0.00	0.00	0.00	0.00	8.31
$i_R$	0.00	0.00	0.00	0.00	0.00	0.00	0.00	0.00	0.00
$i_S$	-60.00	103.92	0.48	-5.76	-14.53	8.07	10.44	6.11	121.88
$i_T$	0.00	0.00	0.00	0.00	0.00	0.00	0.00	0.00	0.00
$\tilde{i}_p$	69.28	0.00	-3.02	1.42	8.23	4.94	0.04	-6.98	70.37
$\tilde{i}_n$	-34.64	-60.00	2.74	1.90	0.16	-9.59	-6.07	3.46	70.37
$\tilde{i}_0$	-34.64	60.00	0.28	-3.32	-8.39	4.65	6.03	3.52	70.37

Table V: Phase-to-neutral and sequence components for current [A] and voltage [V] vectors for problem in Fig. 7.

can be obtained. In this case, the transformation of voltages and currents is presented in Table IV. The corresponding values for the phases and sequences of each harmonic are shown in Table V. Based on the data obtained, the geometrical power results in

$$\begin{aligned} \mathbf{M} = \mathbf{u}\mathbf{i} = & 28,804.56 - 43.54\sigma_{(7)(8)} - 119.65\sigma_{(13)(14)} \\ & - 27.65\sigma_{(19)(20)} + \mathbf{R} \end{aligned}$$

The magnitude of the multivector power is  $\|\mathbf{M}\| = 50,705$ , so the power factor yields  $pf = 28,804/50,705 = 0.568$ . The reactive power components are due to the positive sequence of harmonic 7<sup>th</sup>, negative sequence of harmonic 5<sup>th</sup> and zero sequence of harmonic 3<sup>rd</sup> represented by blades  $\sigma_{(7)(8)}$ ,  $\sigma_{(13)(14)}$  and  $\sigma_{(19)(20)}$ , respectively. The total reactive power in Budeanu sense is  $Q = -43.54 - 119.65 - 27.65 = -190.84$  VAR. The current compensation of the system can be approached as usual, either by a Fryze strategy or by a symmetrical component strategy. For example, the Fryze current can be obtained as

$$\mathbf{i}_a = \frac{\mathbf{u}}{\|\mathbf{u}\|^2} P = 69.19\sigma_1 + 1.04\sigma_7 + 2.08\sigma_{13} + 1.38\sigma_{19}$$

and the norm of the compensated current  $\|\mathbf{i}_a\| = 69.24$  A.

## VI. APPLICATION TO THREE-PHASE REAL-WORLD CASE

As a final example, a real three-phase 4-wire installation in a research building is analyzed, which exhibits an unbalanced and distorted voltage at the source, as well as an unbalanced load. The voltage and current measurements were acquired using the openzmeter device [22], [23], which provides both the raw samples and the frequency phasors of the current and voltage signals. A snapshot of the measured voltage and

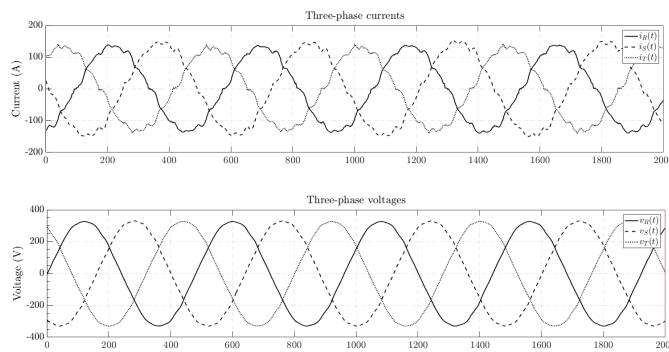


Figure 8: Time domain currents and voltages acquired using the openzmeter device in a research building.

	$\ V\ $	$\ I\ $	$\ M\ $	$P$	$P^+$	$P^-$	$P^0$	$Q$	pf
Original	405.77	167.75	68,069	21,671	21,663	5.18	2.58	64,294	0.32
Positive	405.77	167.36	67,908	21,663	21,663	0.00	0.00	64,307	0.32
Fryze	405.77	53.41	21,671	21,671	21,667	2.89	0.19	0.00	1.00
PHC	405.77	53.35	21,649	21,647	21,647	0.00	0.00	0.00	1.00

Table VI: Main results for the research building example. Different current compensation strategies are shown in each row. PHC stands for Perfect Harmonic Cancellation.

current waveforms is presented in Fig. 8, where slight voltage distortion and significant asymmetry and distortion in the current are observed. To analyze this system, a total of 50 harmonics are considered for the voltage and current signals. They are first transformed into the geometrical domain, and then the sequence components and SC voltage and current vectors are calculated. The proposed method can compute the system's performance and the characteristics of the geometric power flow can be accurately determined. Table VI shows the main results for the different variables involved. The uncompensated geometric current (power) is compared with three compensation strategies: positive only, minimum current with the same active power (Fryze) and Perfect Harmonic Cancellation (PHC). The best results are obtained using Fryze and PHC compensation methods.

## VII. CONCLUSIONS

This research paper presented a novel approach for power definitions and computations in multi-phase AC circuits in the frequency domain using Geometric Algebra. This proposal enables the representation of harmonic voltages and currents as multidimensional vectors in Euclidean space, and the definition of the geometric product to conform to the geometric power. The proposed method provides a generalization and extension of previous works that have focused on single-phase and balanced three-phase systems. The results demonstrate that the GA-based approach can accurately and effectively analyze power flow in arbitrary multi-phase electrical systems, surpassing traditional methods based on complex numbers and matrices. The contribution of this research provides a new geometric foundation for power flow analysis in electrical engineering, with the potential to optimize power system operation and ensure the reliability of the electrical grid. Further research could focus on applying this approach to more complex systems and integrating it with optimal power flow and contingency analysis techniques. It may be possible

to identify more efficient and reliable ways of transmitting and distributing electrical energy, which could have significant practical applications in the field of electrical engineering.

## REFERENCES

- [1] X. Wang, F. Blaabjerg, Harmonic stability in power electronic-based power systems: Concept, modeling, and analysis, *IEEE Transactions on Smart Grid* 10 (3) (2018) 2858–2870.
- [2] A. E. Emanuel, Apparent power definitions for three-phase systems, *IEEE Transactions on Power Delivery* 14 (3) (1999) 767–772.
- [3] J. L. Willems, Reflections on apparent power and power factor in nonsinusoidal and polyphase situations, *IEEE Transactions on Power Delivery* 19 (2) (2004) 835–840.
- [4] J. L. Willems, Budeanu's reactive power and related concepts revisited, *IEEE Transactions on Instrumentation and Measurement* 60 (4) (2010) 1182–1186.
- [5] L. S. Czarnecki, Considerations on the reactive power in nonsinusoidal situations, *IEEE transactions on instrumentation and measurement* (3) (1985) 399–404.
- [6] F. G. Montoya, F. d. León, F. Arrabal-Campos, A. Alcayde, Determination of instantaneous powers from a novel time-domain parameter identification method of non-linear single-phase circuits, *IEEE Transactions on Power Delivery* 37 (5) (2022) 3608–3619. doi: 10.1109/TPWRD.2021.3133069.
- [7] J. Mikulović, B. Škrbić, Ž. Đuričić, Power definitions for polyphase systems based on Fortescue's symmetrical components, *International Journal of Electrical Power & Energy Systems* 98 (2018) 455–462.
- [8] J. Mikulović, T. Šekara, M. Forcan, Power definitions for three-phase systems in terms of instantaneous symmetrical components, *International Journal of Electrical Power & Energy Systems* 147 (2023) 108808.
- [9] P. Filipiński, Apparent power—a misleading quantity in the non-sinusoidal power theory: Are all non-sinusoidal power theories doomed to fail?, *European Transactions on Electrical Power* 3 (1) (1993) 21–26.
- [10] S. Sarabandi, F. Thomas, A survey on the computation of quaternions from rotation matrices, *Journal of mechanisms and robotics* 11 (2) (2019).
- [11] L. Dorst, C. Doran, J. Lasenby, *Applications of geometric algebra in computer science and engineering*, Springer Science & Business Media, 2012.
- [12] F. G. Montoya, A. H. Eid, Formulating the geometric foundation of Clarke, Park, and FBD transformations by means of Clifford's geometric algebra, *Mathematical Methods in the Applied Sciences* 45 (8) (2022) 4252–4277.
- [13] F. G. Montoya, X. Prado, F. M. Arrabal-Campos, A. Alcayde, J. Mira, New mathematical model based on geometric algebra for physical power flow in theoretical two-dimensional multi-phase power circuits, *Scientific Reports* 13 (1) (2023) 1128.
- [14] A. H. Eid, F. G. Montoya, A systematic and comprehensive geometric framework for multiphase power systems analysis and computing in time domain, *IEEE Access* 10 (2022) 132725–132741.
- [15] F. G. Montoya, R. Baños, A. Alcayde, F. M. Arrabal-Campos, Geometric algebra for teaching AC circuit theory, *International Journal of Circuit Theory and Applications* 49 (11) (2021) 3473–3487.
- [16] F. G. Montoya, R. Baños, A. Alcayde, F. M. Arrabal-Campos, J. Roldán-Pérez, Geometric algebra applied to multiphase electrical circuits in mixed time–frequency domain by means of hypercomplex Hilbert transform, *Mathematics* 10 (9) (2022) 1419.
- [17] A. Menti, T. Zacharias, J. Miliadis-Argitis, Geometric algebra: A powerful tool for representing power under nonsinusoidal conditions, *IEEE Transactions on Circuits and Systems I: Regular Papers* 54 (3) (2007) 601–609.
- [18] M. Castilla, J. C. Bravo, M. Ordóñez, J. C. Montaño, Clifford theory: A geometrical interpretation of multivectorial apparent power, *IEEE Transactions on Circuits and Systems I: Regular Papers* 55 (10) (2008) 3358–3367.
- [19] M. Castro-Núñez, R. Castro-Puche, The IEEE standard 1459, the CPC power theory, and geometric algebra in circuits with nonsinusoidal sources and linear loads, *IEEE Transactions on Circuits and Systems I: Regular Papers* 59 (12) (2012) 2980–2990.
- [20] F. G. Montoya, R. Baños, A. Alcayde, F. M. Arrabal-Campos, J. Roldán-Pérez, Vector geometric algebra in power systems: An updated formulation of apparent power under non-sinusoidal conditions, *Mathematics* 9 (11) (2021) 1295.
- [21] F. G. Montoya, R. Baños, A. Alcayde, F. M. Arrabal-Campos, J. Roldán-Pérez, Geometric algebra framework applied to symmetrical balanced three-phase systems for sinusoidal and non-sinusoidal voltage supply, *Mathematics* 9 (11) (2021) 1259.
- [22] E. Vicián, A. Alcayde, F. G. Montoya, R. Baños, F. M. Arrabal-Campos, A. Zapata-Sierra, F. Manzano-Agugliaro, Openzmeter: An efficient low-cost energy smart meter and power quality analyzer, *Sustainability* 10 (11) (2018) 4038.
- [23] E. Vicián, F. M. Arrabal-Campos, A. Alcayde, R. Baños, F. G. Montoya, All-in-one three-phase smart meter and power quality analyzer with extended IoT capabilities, *Measurement* 206 (2023) 112309.